Neurotoxicology 75 (2019) 14–23

Contents lists available at ScienceDirect

Neurotoxicology

journal homepage: www.elsevier.com/locate/neuro

Full Length Article

25-hydroxycholesterol impairs neuronal and muscular development in zebrafish

Priyanka Jamadagni[a], Shunmoogum A. Patten[a,b,*]

[a] INRS Institut Armand-Frappier, Laval, QC, Canada
[b] Centre d'Excellence en Recherche sur les Maladies Orphelines – Fondation Courtois (CERMO-FC), Université du Québec à Montréal (UQAM), Montréal, QC, Canada

ARTICLE INFO

Keywords:
25-hydroxycholesterol
Zebrafish
Neurodevelopment
Behavior
Oxysterol
Neurodegeneration

ABSTRACT

Oxysterols have essential effects on brain homeostasis and their levels are often altered in neurodegenerative and neuroinflammatory diseases. Several studies have demonstrated the cytotoxic effects of 25-HC on different cell lines, however, not much is known about its effects on neurons *in vivo*. In this study, we examined the effects of 25-HC exposure on the nervous system development in the zebrafish. We showed that survival rate of zebrafish embryos/larvae is significantly decreased at doses of 25-HC above 40 μM. 25-HC was found to affect the motility of zebrafish larvae, primary motor axon and muscle morphology. Furthermore, larvae treated with 25-HC showed a reduced neuronal network and number of HuC-positive cells in the brain. An increased cell death was also observed in both the brain and spinal cord of zebrafish treated with 25-HC. Interestingly, administration of 25-HC at later stages of development (24 and 48 h post fertilization) had no detrimental effects on motor axons. Altogether, our findings show that elevated levels of 25-HC may have important consequences on neuronal development and cell survival.

1. Introduction

Cholesterol plays an essential role in the development and maintenance of neuronal development and function. Particularly, it is involved in the biophysical properties of membranes and biogenesis of synapses (Pfrieger, 2003; Zhang and Liu, 2015). As a part of its pathways of function, cholesterol is metabolized to different natural oxysterols including 24-hydroxycholesterol, 25-hydroxycholesterol and 27-hydroxycholesterol (Accad and Farese, 1998; Bjorkhem et al., 1994; Lutjohann et al., 1996; Wolf, 1999). 24-hydroxycholesterol (24-HC) regulates the expression of enzymes involved in brain cholesterol homeostasis (Bjorkhem et al., 1998; Lutjohann et al., 1996). It has recently been shown to be important in midbrain dopaminergic neurogenesis (Theofilopoulos et al., 2019, 2013). 25-hydroxycholesterol (25-HC), on the other hand, is a stronger suppressor of sterol synthesis (Brown and Goldstein, 1974; Peet et al., 1998). It is produced by the enzyme cholesterol 25-hydroxylase (CH25 H) by cells in response to alterations in cholesterol levels and also during infections. It acts as an amplifier of inflammatory responses and has multiple effects on lipid metabolism (Bauman et al., 2009; Gold et al., 2014, 2012; Liu et al., 2013; Ma et al., 2008; Wang et al., 2012). 25-HC regulates the activity of the sterol regulatory element binding proteins (SREBPs) and the liver X receptors (LXRs) signaling pathway by reducing cholesterol synthesis and increasing its efflux and elimination (Accad and Farese, 1998; Radhakrishnan et al., 2007).

Elevated oxysterols production has been implicated in several disease conditions (Jusakul et al., 2011; Kuver, 2012). For instance, the level of 24-HC has been shown to increase in patients with Alzheimer's disease (Kolsch et al., 2003; Papassotiropoulos et al., 2000; Schonknecht et al., 2002). Indeed, the implication of 24-HC in Alzheimer's pathogenesis and neuronal death have been well-documented (Brown et al., 2004; Gamba et al., 2011; Johansson et al., 2004; Papassotiropoulos et al., 2003; Sun et al., 2016; Testa et al., 2016; Yamanaka et al., 2011). 25-HC has also been found at high levels in neurological diseases such as amyotrophic lateral sclerosis (ALS) (Kim et al., 2017), neuromyelitis optica (Cha et al., 2016), spastic paraplegia type 5 (Marelli et al., 2018) and X-linked adrenoleukodystrophy (Jang et al., 2016). An amplified production of 25-HC has been observed upon viral infections (Blanc et al., 2013; Li et al., 2017; Liu et al., 2013; Shrivastava-Ranjan et al., 2016). However, the link between neuronal damage/loss and 25-HC in neurological diseases and/or viral infections is unclear. Interestingly, several reports have shown that 25-HC causes toxicity in different cell lines such as PC12 cells (Chang and Liu, 1997), murin CATH.a neuronal cell line (Waltl et al., 2013) and oligodendrocyte 158 N cell line (Trousson et al., 2009). These findings remain to be validated *in vivo*.

* Corresponding author at: INRS- Institut Armand-Frappier, 531 Boulevard des Prairies, Laval, Quebec, H7V 1B7, Canada.
E-mail address: kessen.patten@iaf.inrs.ca (S.A. Patten).

https://doi.org/10.1016/j.neuro.2019.08.007
Received 28 January 2019; Received in revised form 16 August 2019; Accepted 16 August 2019
Available online 23 August 2019
0161-813X/ © 2019 The Authors. Published by Elsevier B.V. This is an open access article under the CC BY-NC-ND license (http://creativecommons.org/licenses/BY-NC-ND/4.0/).

Zebrafish is a powerful model organism for neurodevelopment and toxicity studies (Hill et al., 2005; Lele and Krone, 1996). They offer unique advantages such as simple, fast, cost-effective, and faithful model for both neurodevelopmental and toxicological studies. The zebrafish cholesterol 25-hydroxylase gene, *ch25hb*, has been identified as the homolog to the mammalian *CH25H* gene *via* synteny, phylogenetic and identity/similarity studies (Pereiro et al., 2017). Also, the nuclear receptor of 25-HC, LXR is highly conserved in zebrafish and has been shown to have a very similar ligand specificity to oxyterols as the human and mouse LXRs (Reschly et al., 2008). The aim of the present study was to explore the effects of 25-HC on the neuronal survival *in vivo* using the zebrafish model. We show that 25-HC affects early neurodevelopment, and motility with an increased cell death in the brain and spinal cord.

2. Materials and methods

2.1. Zebrafish maintenance

Wild-type (AB/TL strain), *isl1*-GFP (Higashijima et al., 2000) and *huc*-GFP (Park et al., 2000) trangenic zebrafish (*Danio rerio*) were bred and maintained according to standard procedures (Westerfield, 1995). For immunohistochemical studies, pigment formation was blocked by adding 0.003% phenylthiourea (PTU) dissolved in egg water at 24 h after fertilization (hpf). All experiments were performed in compliance with the guidelines of the Canadian Council for Animal Care and our local animal care committee.

2.2. 25-hydroxycholesterol treatment and analysis

Embryos were treated with 25-hydroxycholesterol (25-HC; Sigma-Aldrich, St-Louis) at concentrations (2 μM, 5 μM, 10 μM, 20 μM, 40 μM, 50 μM, 60 μM, 80 μM and 100 μM) as of 4 hpf and exposed over four days postfertilization (dpf). The stock of 25-hydroxycholesterol was prepared at 1 mg/ml and stored at − 20 °C. For each experimental trial, embryos were obtained and pooled from the spawning adults held in three mating tanks (2–3 couples/tank) overnight and considered as N = 1. Embryos were treated with different concentrations of 25-hydroxycholesterol in batches of 20 embryous (n = 20), over 10 replicates (N = 10) and quantified for survival, hatching, gross morphological and behavioural changes. For the imaging analyses, each treatment group consisted of n = 7 fish and the tests were repeated 3–4 times (N = 3–4). Experiments for each N were conducted independently on different spawning days. The survival and hatching rates of the embryos were assessed. Brain neuronal morphology following treatments were analyzed in *huc:GFP* and *isl1:GFP* transgenics at 2 dpf. Briefly, 2 dpf zebrafish were fixed in 4% paraformaldehyde overnight at 4 °C and then analyzed for differences using a Zeiss LSM780 confocal microscope. Behavioral responses were also assessed at 20 hpf and 2 dpf.

2.3. Motor activity measurements

20 hpf embryos were embedded in low melting agarose and their movements inside the chorion were recorded using a camera for 20 min during which time they were kept hydrated. The Danioscope software (Noldus) was then used to quantify the percentage of time the embryos were active, the number of coils and coil duration. Behavioral touch responses were also monitored at 2 dpf. Briefly zebrafish larvae were touched lightly at the level of the tail with a pair of blunt forceps and their response to touch was visualized and captured using a Leica S6E stereoscope mounted with a camera, at 60 frames-per-seconds. At later stages (5dpf), larvae were transferred individually into a 96-well plate and activity was recorded over light-dark cycles using Basler GenIcam camera and DanioVision recording chamber (Noldus). Analysis was performed using the Ethovision XT 12 software (Noldus) to quantify the distance swam.

2.4. Motor axonal visualization

Immunohistochemical analyses were performed on 2 dpf zebrafish to visualize axonal projections of motor neurons. The embryos at 2 dpf were fixed in Dents (20% DMSO and 80% Methanol) overnight at 4 °C. After fixation, the embryos were rehydrated with serially decreasing concentrations of Methanol in PBST (75%, 50% and 25%) for 30 min. each and then rinsed several times (1 h) with PBST (0.1% Tween). Following this, embryos were incubated in block solution (2% BSA and 10% NGS in PBST) for 1 h and primary antibody was added to it (anti acetylated tubulin, 1:500, Sigma-Aldrich) and was incubated overnight at 4 °C. The next day, embryos were rinsed with PBST (0.1% Tween) and blocked again for 1 h (2% BSA and 10% NGS in PBST); secondary antibody (Alexa fluor 488, 1:1000, Invitrogen) was then added and incubated overnight at 4 °C as before. Embryos were rinsed the following day with PBST (1 h) again and mounted on a glass slide in 80% glycerol. Z-stack images were taken using a Zeiss LSM 780 confocal microscope.

2.5. Mauthner cell, muscle and α-bungarotoxin staining

Immunohistochemical analyses were performed on 2 dpf zebrafish to visualize the Mauthner cells in the zebrafish hindbrain, muscle morphology and the postsynaptic receptors at the neuromuscular junctions.

Embryos (2 dpf) were fixed in 4% paraformaldehyde (PFA) overnight at 4 °C. After fixation, the embryos were rinsed two times for ten minutes each with PBST (0.1% Tween). Following this, embryos were incubated in collagenase (1 mg/ml in PBS) for 30 min. and then the collagenase was rinsed several times with PBST (0.5% Triton-X). The embryos were then incubated in block solution (2% NGS, 1% BSA, 1% DMSO, 1% Triton) for 1 h and finally the fish were incubated with PBST containing 10ug/ml sulforhodamine-conjugated α bungarotoxin (Molecular Probes), which binds irreversibly to acetylcholine receptors, for 30 min. The embryos were then rinsed several times with PBST (0.5% Triton-X) and then imaged.

For visualization of muscles using phalloidin staining, embryos were fixed as above, followed by permeabilization in 2% Triton X-100/PBS for 1.5 h and incubation in 1:20 Alexa-Fluor 488 conjugated phalloidin (Invitrogen) overnight at 4 °C on a mild shaker. Embryos were then rinsed and imaged.

For Mauthner cells staining, after fixation, the embryos were rinsed multiple times with PBST (0.5% Triton-X) followed by dH_2O – triton-X (0.5%). They were then incubated acetone (100%) at – 20 °C for 10 min. Following this the embryos were rinsed with PBST (0.5% Triton-X) and PBS-DT (1% BSA, 1% DMSO, 0.5% Triton-X) and further blocked in 5% NGS in PBS-DT for 1 h. Primary antibody (anti-3A10, 1:200; The Developmental Studies Hybridoma Bank, University of Iowa) was added to the blocking solution and incubated overnight at 4 °C. The next day, embryos were rinsed with PBS-DT and secondary antibody (Alexa fluor 488, 1:1000; Invitrogen) was then added and incubated overnight at 4 °C as before. Embryos were rinsed and imaged with a Zeiss LSM 780 confocal microscope.

2.6. TUNEL staining

2 dpf fish were fixed in 4% PFA and then serially dehydrated and rehydrated with 25, 50 and 75% MeOH in PBST (0.1% Tween) and rinsed with PBST several times. The embryos were then digested with Proteinase K (10 μg/ml) for 20 min., followed by rinses with PBST and re-fixed with 4% PFA for 20 min. This was followed by 2 quick washes and 3 long washes of 20 min. in PBST (1% Triton-X), then were rinsed again with PBS and incubated in TUNEL reaction mix (as directed by the manufacturers; Sigma-Aldrich) for 1 h at 37 °C. The embryos were then mounted and imaged under a Zeiss LSM 780 confocal microscope.

2.7. Acridine Orange staining

Embryos at 48 hpf were placed in independent wells of a 6 well plate with Acridine Orange (Sigma-Aldrich) at room temperature with Acridine Orange 1X for 30 min in E3 medium. Acridine Orange stock was prepared at 1 mg/ml (100X) in milliQ water and stored at -20C (light protected). The embryos were then washed 3 times for 10 min with E3 medium. They were then treated with tricaine and dead cells were visualised under a Nikon, Eclipse Ti-S compound microscope.

2.8. Late 25-HC exposure treatments

Zebrafish at 24 hpf and 2 dpf were also treated overnight with 25-HC (10 μM and 40 μM) to assess the effects of 25-HC at later stages once major developmental processes have taken place. Following, 25-HC treatments, the larvae were assessed for cell death and neuronal defects.

2.9. Statistical analysis

All data values are given as means ± S.E.M. Signicance was determined using One-way ANOVA followed by a Tukey post-hoc multiple comparisons test for normally distributed and equal variance data. Kruskal-Walllis ANOVA and Dunn's method of comparison were used for non-normal distributions. Statistical analysis was done using GraphPad prism.

3. Results

3.1. 25-hydroxycholesterol (25-HC) affects development and is lethal upon chronic exposure at higher doses

Zebrafish embryos (2–4 cell-stage) were treated with a range of nine concentrations of 25-HC- 2, 5, 10, 20, 40, 50, 60, 80, 100 μM over a period of 4 days and analyzed daily for their survival rate, hatching rate and gross morphology. Effects of 25-HC exposure on survival rate, hatching rate and morphology in zebrafish embryos-larvae are shown in Fgure 1. Compared to controls, no significant change in mortality was observed at 24–96 hpf for 2–40 μM 25-HC treatment groups. However, survival rates were significantly decreased at high doses of 25-HC (50–100 μM) leading to death in 100% of the embryos at as early as 2 dpf in 80 μM and 100 μM treatment groups (Fig. 1A). Embryos exposed to 25-HC treatments caused visible morphological defects like a curved spine and mild to extreme pericardial edema, but no apparent change in the whole body size at 0–40 μM (Fig. 1C). Total morphological defect rates were increased in the 40 μM 25-HC group and beyond. At higher concentrations beyond 40 μM the embryos died at two- and three-days post fertlization deeming it impossible to use them for early developmental studies (Fig. 1A). Hatching rates were not significantly affected upon 25-HC exposure up to 40 μM concentration (Fig. 1B). Thus, in order to further investigate the effects of 25-HC on the zebrafish nervous system during early developmental stages, a representative low and high dose (10 μM and 40 μM) at which the embryos survived with relatively consistent developmental effects were chosen in the follow-up study.

3.2. 25-HC affects early motility in zebrafish larvae

To assess for any impact of chronic exposure of 25-HC on the nervous system, we first evaluated motor behaviours of zebrafish embryos and larvae. Interestingly, early spontaneous coiling of the embryos showed a decreasing trend with a significantly low coiling at 40 μM (Fig. 2A). A similar aberrant motor behavior was also observed at 2 dpf, where, in a touch-evoked swimming response of the larvae exposed to 10 and 40 μM 25-HC, the larvae exposed to 40 μM concentration barely moved upon being touched (Fig. 2C). At 5 dpf, we observed a significantly decreased in motor activity in larvae treated with 10 μM 25-HC and no motility in fish exposure chronically to 40 μM 25-HC (Fig. 2B). Besides the motility defects, zebrafish larvae exposed to 40 μM 25-HC displayed abnormally shortened motor neuron axonal processes (Fig. 3A). Additionally, the 40 μM 25-HC treatment disrupted neuromuscular junctions (Fig. 3B) and muscle morphologies (Fig. 3C). Specifically, we observed an abnormal clustering of postsynaptic receptors at the middle of the each somite (Fig. 3B, marked by arrows). Larvae exposed to a lower concentration of 25-HC had no significant difference in motor axonal morphology (Fig. 3A), number of postsynaptic receptors at neuromuscular junctions (Fig. 3B) and muscle morphology (Fig. 3C) compared to controls. We did not observe major changes in the morphology of the Mauthner cells (Supplementary Fig. 1A). This data suggest that high levels of 25-HC may have severe consequences on early development of the motor system primarily at the motor axon level.

3.3. 25-HC alters central nervous system development in zebrafish and results in cell death

We next sought to further assess the effects of elevated levels of 25-HC on the central nervous system. To do so, we took advantage of the [huc:GFP] transgenic line that expresses GFP in all post-mitotic neurons. The comparison of the general structure of the larval brain at 2 dpf showed a decrease in head size (Fig. 4A) and a decrease in the neuronal population in the brain, more distinctly at 40 μM than at 10 μM (Fig. 4B).

We next examined the cranial motor neurons in the zebrafish larvae exposed to 25-HC using the [*isl1*:GFP] transgenic line. Zebrafish administered with 40 μM 25-HC exhibited a severe reduction in position and number of trigeminal (nV) and facial (nVII) branchiomotor neuron populations at 2 dpf compared to controls. Furthermore, in these fish the vagal (nX) motor neurons displayed aberrant medio-lateral positioning and cell-to-cell spacing (Fig. 4D). Although, zebrafish exposed to 10 μM 25-HC exhibited an abnormal positioning of facial (nVII) branchiomotor neuron populations, these defects were less severe compared to fish exposed to a higher level of 25-HC (Fig. 4D). We also analyzed the cranial axons using an acetylated tubulin marker that stains mature neurites. Treatment with 25-HC led to an overall decrease in the number of cranial axons. At the higher dose, staining with acetylated tubulin is nearly abolished in axons of the optic tectum and trigeminal ganglion cells (Fig. 4C). 25-HC exposure led to a significant increase in apoptotic cells in both the brain and spinal cord and in a dose dependent manner, as compared to untreated larvae (Fig. 5, Supplementary Fig. 1B, C).

3.4. Late exposure to 25-HC had no effect on zebrafish neurodevelopment

We next tested whether 25-HC-induced defects are dependent on the stage of development at which administered. Zebrafish embryos were treated with 25-HC at 24 hpf and 2 dpf and analysed at 2 dpf and 3 dpf respectively for any anomalies. Interestingly, no significant death or alteration in motor axonal features was observed if 25-HC is administered after 24 hpf or 2 dpf, when many development processes have initiated or occurred (Supplementary Figs. 2 and 3B). However, the axonal neural network in the brain is more disorganized in 25-HC treated fish compared to controls (Supplementary Fig. 3A).

4. Discussions

Several studies have reported the toxicity effects of exogenously added 25-HC *in vitro* (Chang and Liu, 1997; Trousson et al., 2009; Waltl et al., 2013). However, the cellular effects of 25-HC remain to be assessed *in vivo*. In the present study, we explored the effects of 25-HC on the nervous system *in vivo* using the zebrafish model. We showed that 25-HC affects early neurodevelopment and motility with an increased cell death in the brain and spinal cord. Late administration of 25-HC

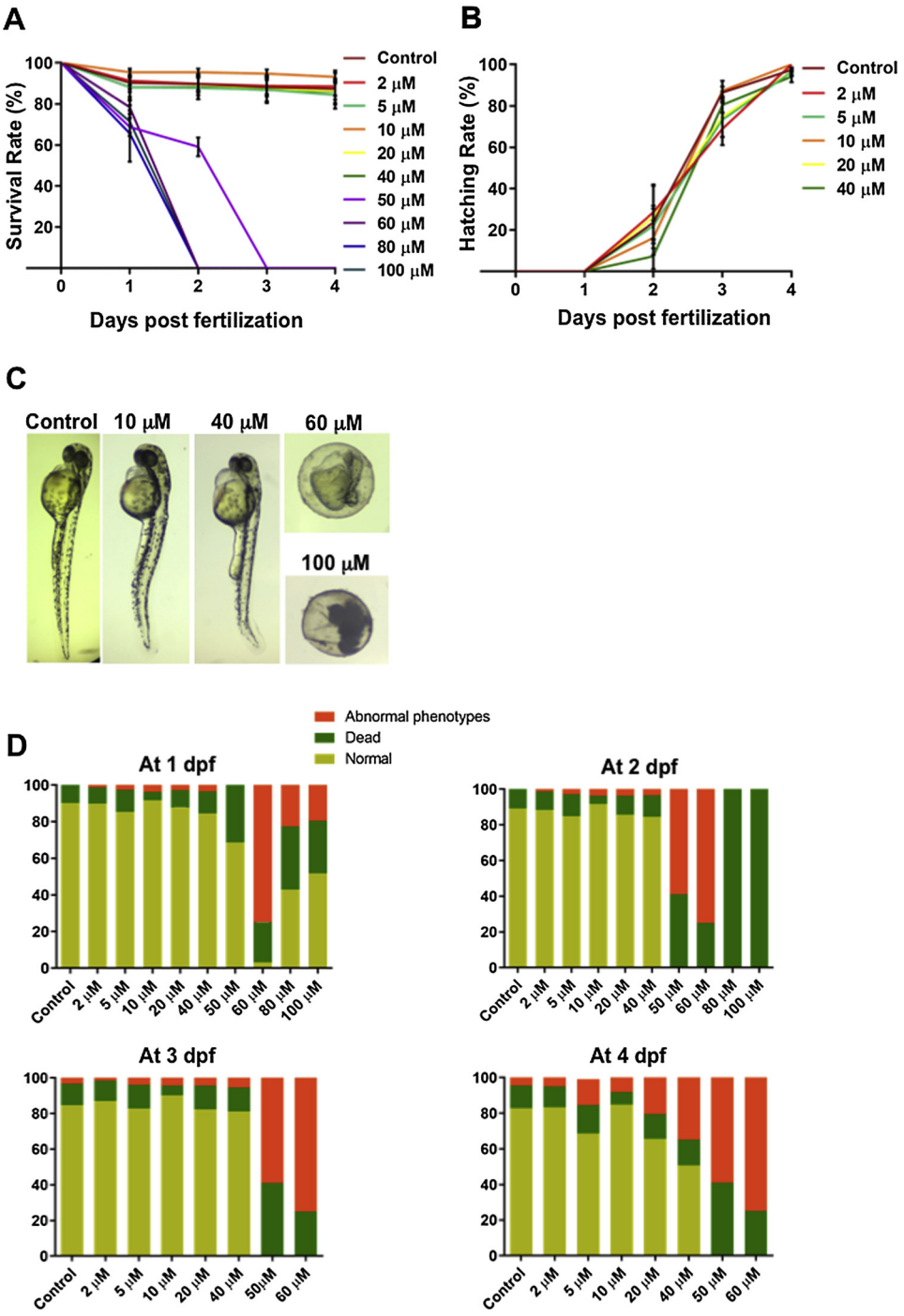

Fig. 1. 25 Hydroxycholesterol affects development and is lethal upon chronic exposure at higher doses: The percentage of embryos surviving decreases (A) and hatching among the surviving embryos is delayed (B) with increase in the concentration of 25 − HC. (C) morphological defects in development of the embryos at 2 dpf (days post fertilization), viewed and imaged using a bright field microscope. Defects get severe with increasing concentration of 25-HC. (D) The percentage of dead embryos and larvae with abnormal phenotypes (with heart edema and curved tails) increases in a dose dependent manner upon chronic exposure.

had no major impact on the zebrafish nervous system.

25-HC is a known ligand of the nuclear receptors, LXRs (Janowski et al., 1999) that play important roles in multiple metabolic pathways (Hong and Tontonoz, 2014; Korach-Andre and Gustafsson, 2015). It also acts as an inverse agonist for the retinoid-related orphan receptor alpha (RORα) (Bitsch et al., 2003; Fitzsimmons et al., 2012; Tuong et al., 2016). RORα has been shown to play an essential role in the development of the central nervous system (Dussault et al., 1998; Hamilton et al., 1996). For example, RORα-deficient mice exhibit the cerebellar developmental defects and an impaired motor coordination (Hamilton et al., 1996). A reduction of neurons in the zebrafish brain upon exposure to 25-HC could very likely be the results of its antagonist effect on RORα and the hampering of its function during neurodevelopment. Moreover, 25-OH can cause alterations of the cytoskeletal organization (Olivier et al., 2017) and this could plausible explain the neuronal network defects observed in the 25-HC treated zebrafish.

In our study, in addition to neuronal defects, we also observed an increased cell death upon 25-HC treatment in zebrafish brain and spinal cord. This observation is consistent with the cytotoxic effects of 25-HC reports in several *in vitro* studies. Engel and colleagues (Engel et al.,

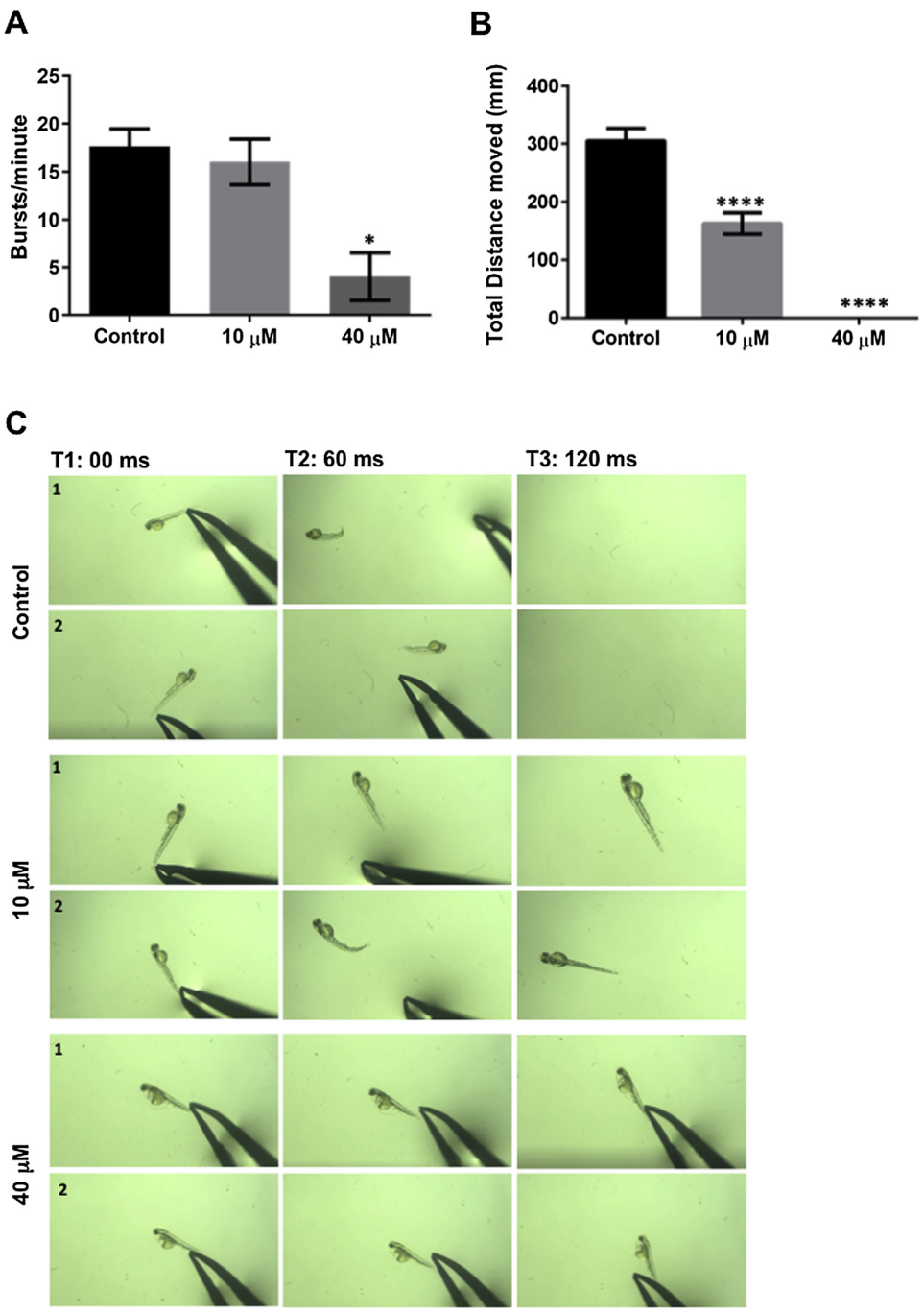

Fig. 2. 25-HC affects early motility in zebrafish larvae: (A) Representation of the number of early spontaneous coiling of the larvae at 20 hpf (hours post fertilization) treated with 25-HC. There is a decrease in a dose dependent manner. (B) The distance moved by 5 dpf larvae upon treatment with 25-HC were assessed using the Ethiovision software, show a highly significant reduction in a dose dependent manner. (C) The figure represents motion snapshots of touch response in two representative trials (1,2) (N = 10) over 120 miliseconds (ms). At 40 μM, the larvae also have very little to no escape response to touch at 2 dpf. All comparisons are performed with control, each trial has a N of 7 for control and treated over 4 trials. * represents a significance of $p < 0.05$, **** represents a significance of $p < 0.01$. Significance was determined using one-way ANOVA and all data are represented as Mean ± SEM.

2014) demonstrated that 25-HC can trigger reactive oxygen species production. Furthermore, 25-HC has been reported to regulate the expression of inflammatory factors such as cytokines (Gueguen et al., 2001; Koarai et al., 2012). It is possible that cell death upon 25-HC treatment in zebrafish is mediated by the stimulation of inflammation or oxidative stress. Interestingly, several neurological defects such as brain lesions, cognitive impairement, axonopathy of the spinal cord, motor dysfunction are associated with childhood X-linked adrenoleukodystrophy (Engelen et al., 2012; Liberato et al., 2019). In these patients, an aberrant elevated production of CH25H and 25-HC has been demonstrated (Jang et al., 2016). It has also been shown that 25-HC mediates the neuroinflammation of X-ALD and neuronal cell death *via* activation of the NLRP3 inflammasome (Jang et al., 2016). Importantly, also 25-HC production is amplified upon virus infection and recent studies have shown that 25-HC can inhibit infection by various pathogenic viruses (Blanc et al., 2013; Li et al., 2017; Liu et al., 2013; Shrivastava-Ranjan et al., 2016) including Zika virus (Li et al., 2017). It thus possible that the neurological defects and cell death observed in zebrafish upon 25-HC treatments could be due to inflammatory reponses and this warrants further investigations. Our findings also raise the concern of the consequences of a viral infection and elevated 25-HC levels during human embryonic development, particularly in the case of Zika virus infection and the associated brain defects.

In this study, we showed that 25-HC treatments resulted in abnormal motor neuron morphology and impaired zebrafish motility. Additionally, we found that exposure to 25-HC also affects neuromuscular junctions and muscles morphology. Interestingly, similar aberrant motor axonal and behavioural phenotypes have been observed in zebrafish models of ALS as early as 2 dpf (Kabashi et al., 2010; Patten et al., 2014). 25-HC has been reported to be present at higher levels in the

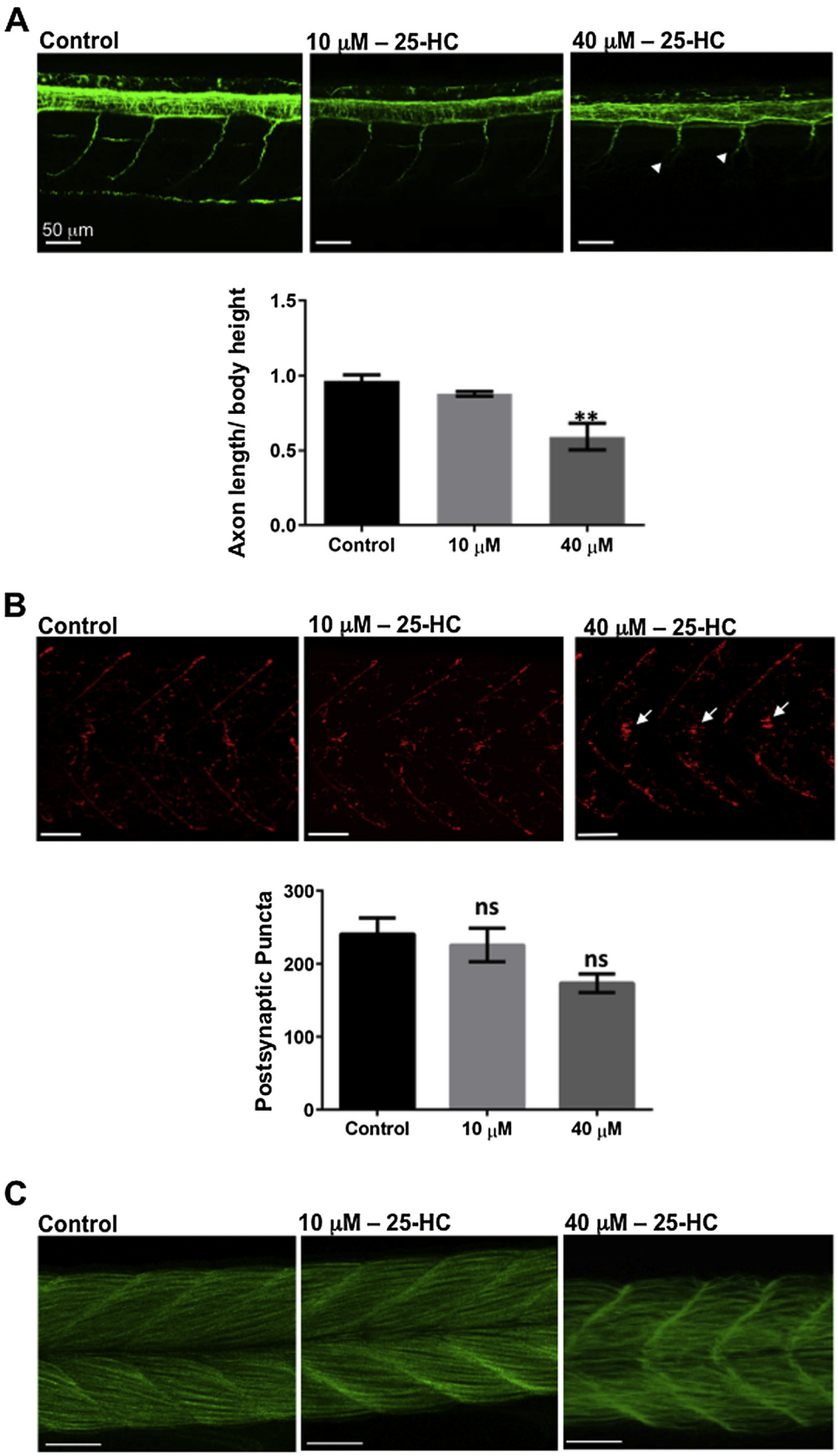

Fig. 3. Effects of 25-HC on the neuromuscular system in zebrafish larvae: (A) The spinal cord of control and treated larvae at 2 dpf, stained for acetylated α-tubulin, showed a significant reduction in the axon length of the motor neurons (white arrow heads) at 40 μM. (B) Staining for α-bungarotoxin in the muscles of treated and control larvae show no significant difference in the number of post-synaptic puncta. (C) Phalloidin staining of muscles in 25-HC-treated fish and controls at 2 dpf. All comparisons are performed with control, each trial has a n of 7 for control and treated over 4 trials. ** represents a significance of $p < 0.01$, ns: not significant. Significance was determined using one-way ANOVA and all data are represented as Mean ± SEM.

serum and cerebrospinal fluid (CSF) of patients with ALS (Kim et al., 2017). Kim and colleagues (Kim et al., 2017) also demonstrated that 25-HC can induce motor neuron death *via* glycogen synthase kinase-3β and LXR pathways; suggesting a possible involvement of 25-HC in ALS pathogenesis. Additionally, altered levels of 25-HC and cholestenoic acid have been observed in SPG5 (Marelli et al., 2018; Schols et al., 2017), a neurological diseases that is characterized by progressive lower limb spasticity and weakness due to degeneration of motor

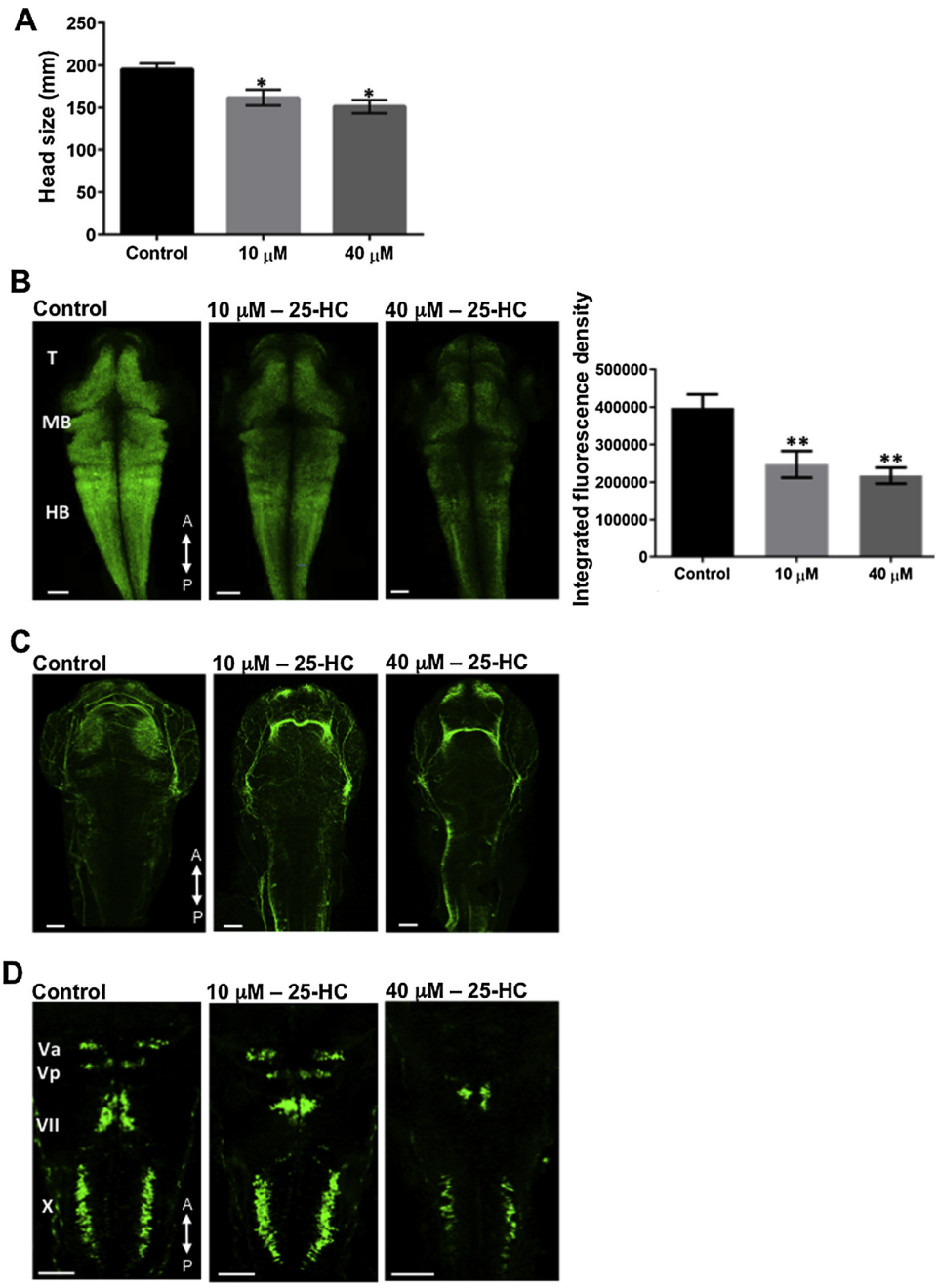

Fig. 4. 25-HC administration alters brain development in zebrafish: (A) Head size comparison between the treated and un-treated larvae at 2 dpf. Characterizing the larval brains at 2 dpf using Tg(*huc*:GFP) (B) and Tg(*Isl1*:GFP) (D) lines showed a decrease in the neuronal population and a defective development of the cranial nerves, in a dose dependent manner. (C) Larvae stained for acetylated α-tubulin at 2 dpf, showed reduced axon network clusters in the brain. All comparisons are performed with control, each trial has a n of 7 for control and treated over 4 trials, * represents a significance of $p < 0.05$, ** represents a significance of $p < 0.01$. Significance was determined using one-way ANOVA and all data are represented as Mean ± SEM. T: Telencephalon, MB: Midbrain, HB, Hindbrain. A, P represent anterior and posterior side of the head respectively.

neurons. Interestingly, it has been previously demonstrated that cholestenoic acid exerts toxic effects in mice and zebrafish motor neurons *via* activation of neuronal LXR receptors (Theofilopoulos et al., 2014). It is thus very plausible that 25-HC may indeed be involved in the pathogenesis of ALS and SPG5 by impacting motor circuitry functioning and motor neuron survival. Although, we did not observe detrimental effects of 25-HC on zebrafish motor axons upon its administration at later developmental stages, it is likely that higher doses of 25-HC are required to impair the functioning and survival of mature motor neurons. Nevertheless, further investigations are required to determine whether an amplified production of 25-HC and motor circuit dysfunction and/or motor neuron degeneration in ALS are directly correlated or a mere coincidental response to the disease. Furthermore, it remains to be determined whether in our model the muscle defects are due to a direct cause of 25-HC or due to consequences of motor neuron defects and loss of muscle innervation.

In summary, our study demonstrated adverse effects of 25-HC on neuromuscular development, survival and behaviour in zebrafish. This study provide new information on the toxic actions of the oxysterol 25-HC on neuronal and muscular development. However, additional tests will be needed to completely characterize the mechanisms by 25-HC lead to these defects. For instance, targeting the binding partners of 25-HC such as LXRs genetically or pharmacologically could also be tested in zebrafish to assess the potential of alleviate effects from 25-HC. Importantly, further validation of the our findings on other models system such as mice is required prior to assessing whether inhibiting 25-HC production could be possibly neuroprotective in certain pathologies.

Declaration of Competing Interest

None.

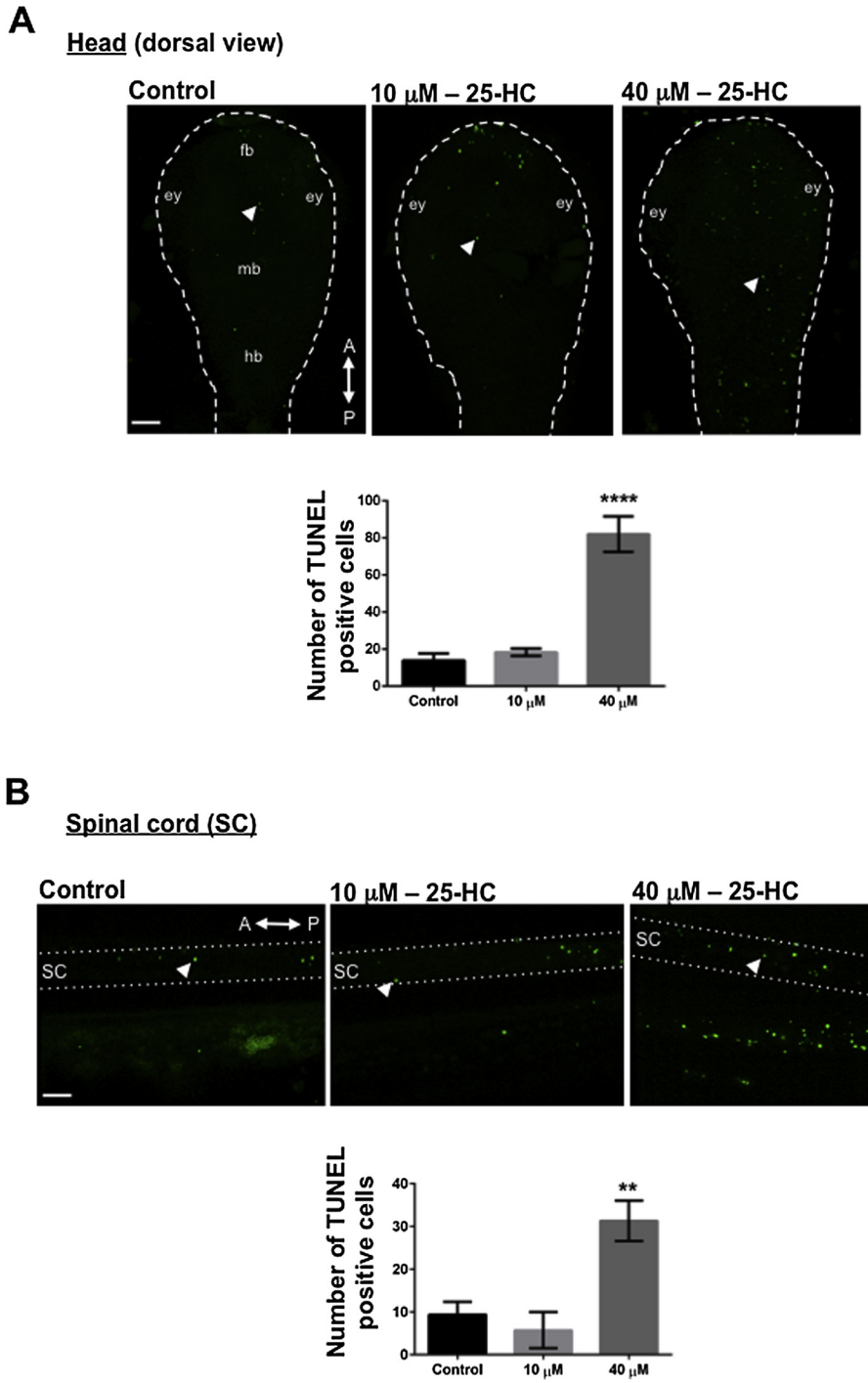

Fig. 5. 25-HC administration causes increased cell death: TUNEL staining at 2 dpf in treated and untreated larvae showed an increased cell death in the head (white arrow heads) (A) and the spinal cord (SC; white arrow heads) (B) upon 25-HC treatment in a dose dependent manner. Ey: eye; fb:forebrain; mb: midbrain; hb: hindbrain; sc: spinal cord. Each trial has a n of 7 for control and treated, repeated over 3 trials. A,P: Anterior and posterior side of the embryos respectively.

Acknowledgements

SP is supported by the Natural Science and Engineering Research Council (NSERC), Canadian Foundation for Innovation (CFI) and an ALS Canada-Brain Canada Career Transition Award. PJ is supported by a CERMO-FC scholarship.

Appendix A. Supplementary data

Supplementary material related to this article can be found, in the online version, at doi:https://doi.org/10.1016/j.neuro.2019.08.007.

References

Accad, M., Farese Jr., R.V., 1998. Cholesterol homeostasis: a role for oxysterols. Curr. Biol. 8 (17), R601–604.
Bauman, D.R., Bitmansour, A.D., McDonald, J.G., Thompson, B.M., Liang, G., Russell, D.W., 2009. 25-hydroxycholesterol secreted by macrophages in response to Toll-like receptor activation suppresses immunoglobulin A production. Proc. Natl. Acad. Sci. U. S. A. 106 (39), 16764–16769.
Bitsch, F., Aichholz, R., Kallen, J., Geisse, S., Fournier, B., Schlaeppi, J.M., 2003. Identification of natural ligands of retinoic acid receptor-related orphan receptor alpha ligand-binding domain expressed in Sf9 cells—A mass spectrometry approach. Anal. Biochem. 323 (1), 139–149.
Bjorkhem, I., Andersson, O., Diczfalusy, U., Sevastik, B., Xiu, R.J., Duan, C., Lund, E.,

1994. Atherosclerosis and sterol 27-hydroxylase: evidence for a role of this enzyme in elimination of cholesterol from human macrophages. Proc. Natl. Acad. Sci. U. S. A. 91 (18), 8592–8596.
Bjorkhem, I., Lutjohann, D., Diczfalusy, U., Stahle, L., Ahlborg, G., Wahren, J., 1998. Cholesterol homeostasis in human brain: turnover of 24S-hydroxycholesterol and evidence for a cerebral origin of most of this oxysterol in the circulation. J. Lipid Res. 39 (8), 1594–1600.
Blanc, M., Hsieh, W.Y., Robertson, K.A., Kropp, K.A., Forster, T., Shui, G., Lacaze, P., Watterson, S., Griffiths, S.J., Spann, N.J., Meljon, A., Talbot, S., Krishnan, K., Covey, D.F., Wenk, M.R., Craigon, M., Ruzsics, Z., Haas, J., Angulo, A., Griffiths, W.J., Glass, C.K., Wang, Y., Ghazal, P., 2013. The transcription factor STAT-1 couples macrophage synthesis of 25-hydroxycholesterol to the interferon antiviral response. Immunity 38 (1), 106–118.
Brown 3rd, J., Theisler, C., Silberman, S., Magnuson, D., Gottardi-Littell, N., Lee, J.M., Yager, D., Crowley, J., Sambamurti, K., Rahman, M.M., Reiss, A.B., Eckman, C.B., Wolozin, B., 2004. Differential expression of cholesterol hydroxylases in Alzheimer's disease. J. Biol. Chem. 279 (33), 34674–34681.
Brown, M.S., Goldstein, J.L., 1974. Suppression of 3-hydroxy-3-methylglutaryl coenzyme A reductase activity and inhibition of growth of human fibroblasts by 7-ketocholesterol. J. Biol. Chem. 249 (22), 7306–7314.
Cha, E., Lee, K.M., Park, K.D., Park, K.S., Lee, K.W., Kim, S.M., Lee, J., 2016. Hydroxycholesterol levels in the serum and cerebrospinal fluid of patients with neuromyelitis optica revealed by LC-Ag+CIS/MS/MS and LC-ESI/MS/MS with picolinic derivatization: increased levels and association with disability during acute attack. PLoS One 11 (12), e0167819.
Chang, J.Y., Liu, L.Z., 1997. 25-Hydroxycholesterol causes death but does not prevent nerve growth factor-induced neurite outgrowth in PC12 cells. Neurochem. Int. 31 (4), 517–523.
Dussault, I., Fawcett, D., Matthyssen, A., Bader, J.A., Giguere, V., 1998. Orphan nuclear receptor ROR alpha-deficient mice display the cerebellar defects of staggerer. Mech. Dev. 70 (1–2), 147–153.
Engel, T., Fobker, M., Buchmann, J., Kannenberg, F., Rust, S., Nofer, J.R., Schurmann, A., Seedorf, U., 2014. 3beta, 5alpha, 6beta-cholestanetriol and 25-hydroxycholesterol accumulate in ATP-binding cassette transporter G1 (ABCG1)-deficiency. Atherosclerosis 235 (1), 122–129.
Engelen, M., Kemp, S., de Visser, M., van Geel, B.M., Wanders, R.J., Aubourg, P., Poll-The, B.T., 2012. X-linked adrenoleukodystrophy (X-ALD): clinical presentation and guidelines for diagnosis, follow-up and management. Orphanet J. Rare Dis. 7, 51.
Fitzsimmons, R.L., Lau, P., Muscat, G.E., 2012. Retinoid-related orphan receptor alpha and the regulation of lipid homeostasis. J. Steroid Biochem. Mol. Biol. 130 (3–5), 159–168.
Gamba, P., Leonarduzzi, G., Tamagno, E., Guglielmotto, M., Testa, G., Sottero, B., Gargiulo, S., Biasi, F., Mauro, A., Vina, J., Poli, G., 2011. Interaction between 24-hydroxycholesterol, oxidative stress, and amyloid-beta in amplifying neuronal damage in Alzheimer's disease: three partners in crime. Aging Cell 10 (3), 403–417.
Gold, E.S., Diercks, A.H., Podolsky, I., Podyminogin, R.L., Askovich, P.S., Treuting, P.M., Aderem, A., 2014. 25-Hydroxycholesterol acts as an amplifier of inflammatory signaling. Proc. Natl. Acad. Sci. U. S. A. 111 (29), 10666–10671.
Gold, E.S., Ramsey, S.A., Sartain, M.J., Selinummi, J., Podolsky, I., Rodriguez, D.J., Moritz, R.L., Aderem, A., 2012. ATF3 protects against atherosclerosis by suppressing 25-hydroxycholesterol-induced lipid body formation. J. Exp. Med. 209 (4), 807–817.
Gueguen, Y., Bertrand, P., Ferrari, L., Batt, A.M., Siest, G., 2001. Control of apolipoprotein E secretion by 25-hydroxycholesterol and proinflammatory cytokines in the human astrocytoma cell line CCF-STTG1. Cell Biol. Toxicol. 17 (3), 191–199.
Hamilton, B.A., Frankel, W.N., Kerrebrock, A.W., Hawkins, T.L., FitzHugh, W., Kusumi, K., Russell, L.B., Mueller, K.L., van Berkel, V., Birren, B.W., Kruglyak, L., Lander, E.S., 1996. Disruption of the nuclear hormone receptor RORalpha in staggerer mice. Nature 379 (6567), 736–739.
Higashijima, S., Hotta, Y., Okamoto, H., 2000. Visualization of cranial motor neurons in live transgenic zebrafish expressing green fluorescent protein under the control of the islet-1 promoter/enhancer. J. Neurosci. 20 (1), 206–218.
Hill, A.J., Teraoka, H., Heideman, W., Peterson, R.E., 2005. Zebrafish as a model vertebrate for investigating chemical toxicity. Toxicol. Sci. 86 (1), 6–19.
Hong, C., Tontonoz, P., 2014. Liver X receptors in lipid metabolism: opportunities for drug discovery. Nat. Rev. Drug Discov. 13 (6), 433–444.
Jang, J., Park, S., Jin Hur, H., Cho, H.J., Hwang, I., Pyo Kang, Y., Im, I., Lee, H., Lee, E., Yang, W., Kang, H.C., Won Kwon, S., Yu, J.W., Kim, D.W., 2016. 25-hydroxycholesterol contributes to cerebral inflammation of X-linked adrenoleukodystrophy through activation of the NLRP3 inflammasome. Nat. Commun. 7, 13129.
Janowski, B.A., Grogan, M.J., Jones, S.A., Wisely, G.B., Kliewer, S.A., Corey, E.J., Mangelsdorf, D.J., 1999. Structural requirements of ligands for the oxysterol liver X receptors LXRalpha and LXRbeta. Proc. Natl. Acad. Sci. U. S. A. 96 (1), 266–271.
Johansson, A., Katzov, H., Zetterberg, H., Feuk, L., Johansson, B., Bogdanovic, N., Andreasen, N., Lenhard, B., Brookes, A.J., Pedersen, N.L., Blennow, K., Prince, J.A., 2004. Variants of CYP46A1 may interact with age and APOE to influence CSF Abeta42 levels in Alzheimer's disease. Hum. Genet. 114 (6), 581–587.
Jusakul, A., Yongvanit, P., Loilome, W., Namwat, N., Kuver, R., 2011. Mechanisms of oxysterol-induced carcinogenesis. Lipids Health Dis. 10, 44.
Kabashi, E., Lin, L., Tradewell, M.L., Dion, P.A., Bercier, V., Bourgouin, P., Rochefort, D., Bel Hadj, S., Durham, H.D., Vande Velde, C., Rouleau, G.A., Drapeau, P., 2010. Gain and loss of function of ALS-related mutations of TARDBP (TDP-43) cause motor deficits in vivo. Hum. Mol. Genet. 19 (4), 671–683.
Kim, S.M., Noh, M.Y., Kim, H., Cheon, S.Y., Lee, K.M., Lee, J., Cha, E., Park, K.S., Lee, K.W., Sung, J.J., Kim, S.H., 2017. 25-Hydroxycholesterol is involved in the pathogenesis of amyotrophic lateral sclerosis. Oncotarget 8 (7), 11855–11867.
Koarai, A., Yanagisawa, S., Sugiura, H., Ichikawa, T., Kikuchi, T., Furukawa, K., Akamatsu, K., Hirano, T., Nakanishi, M., Matsunaga, K., Minakata, Y., Ichinose, M., 2012. 25-Hydroxycholesterol enhances cytokine release and Toll-like receptor 3 response in airway epithelial cells. Respir. Res. 13, 63.
Kolsch, H., Lutjohann, D., von Bergmann, K., Heun, R., 2003. The role of 24S-hydroxycholesterol in Alzheimer's disease. J. Nutr. Health Aging 7 (1), 37–41.
Korach-Andre, M., Gustafsson, J.A., 2015. Liver X receptors as regulators of metabolism. Biomol. Concepts 6 (3), 177–190.
Kuver, R., 2012. Mechanisms of oxysterol-induced disease: insights from the biliary system. Clin. Lipidol. 7 (5), 537–548.
Lele, Z., Krone, P.H., 1996. The zebrafish as a model system in developmental, toxicological and transgenic research. Biotechnol. Adv. 14 (1), 57–72.
Li, C., Deng, Y.Q., Wang, S., Ma, F., Aliyari, R., Huang, X.Y., Zhang, N.N., Watanabe, M., Dong, H.L., Liu, P., Li, X.F., Ye, Q., Tian, M., Hong, S., Fan, J., Zhao, H., Li, L., Vishlaghi, N., Buth, J.E., Au, C., Liu, Y., Lu, N., Du, P., Qin, F.X., Zhang, B., Gong, D., Dai, X., Sun, R., Novitch, B.G., Xu, Z., Qin, C.F., Cheng, G., 2017. 25-hydroxycholesterol protects host against zika virus infection and its associated microcephaly in a mouse model. Immunity 46 (3), 446–456.
Liberato, A.P., Mallack, E.J., Aziz-Bose, R., Hayden, D., Lauer, A., Caruso, P.A., Musolino, P.L., Eichler, F.S., 2019. MRI brain lesions in asymptomatic boys with X-linked adrenoleukodystrophy. Neurology 92 (15), e1698–e1708.
Liu, S.Y., Aliyari, R., Chikere, K., Li, G., Marsden, M.D., Smith, J.K., Pernet, O., Guo, H., Nusbaum, R., Zack, J.A., Freiberg, A.N., Su, L., Lee, B., Cheng, G., 2013. Interferon-inducible cholesterol-25-hydroxylase broadly inhibits viral entry by production of 25-hydroxycholesterol. Immunity 38 (1), 92–105.
Lutjohann, D., Breuer, O., Ahlborg, G., Nennesmo, I., Siden, A., Diczfalusy, U., Bjorkhem, I., 1996. Cholesterol homeostasis in human brain: evidence for an age-dependent flux of 24S-hydroxycholesterol from the brain into the circulation. Proc. Natl. Acad. Sci. U. S. A. 93 (18), 9799–9804.
Ma, Y., Xu, L., Rodriguez-Agudo, D., Li, X., Heuman, D.M., Hylemon, P.B., Pandak, W.M., Ren, S., 2008. 25-Hydroxycholesterol-3-sulfate regulates macrophage lipid metabolism via the LXR/SREBP-1 signaling pathway. Am. J. Physiol. Endocrinol. Metab. 295 (6), E1369–1379.
Marelli, C., Lamari, F., Rainteau, D., Lafourcade, A., Banneau, G., Humbert, L., Monin, M.L., Petit, E., Debs, R., Castelnovo, G., Ollagnon, E., Lavie, J., Pilliod, J., Coupry, I., Babin, P.J., Guissart, C., Benyounes, I., Ullmann, U., Lesca, G., Thauvin-Robinet, C., Labauge, P., Odent, S., Ewenczyk, C., Wolf, C., Stevanin, G., Hajage, D., Durr, A., Goizet, C., Mochel, F., 2018. Plasma oxysterols: biomarkers for diagnosis and treatment in spastic paraplegia type 5. Brain 141 (1), 72–84.
Olivier, E., Dutot, M., Regazzetti, A., Dargere, D., Auzeil, N., Laprevote, O., Rat, P., 2017. Lipid deregulation in UV irradiated skin cells: role of 25-hydroxycholesterol in keratinocyte differentiation during photoaging. J. Steroid Biochem. Mol. Biol. 169, 189–197.
Papassotiropoulos, A., Lutjohann, D., Bagli, M., Locatelli, S., Jessen, F., Rao, M.L., Maier, W., Bjorkhem, I., von Bergmann, K., Heun, R., 2000. Plasma 24S-hydroxycholesterol: a peripheral indicator of neuronal degeneration and potential state marker for Alzheimer's disease. Neuroreport 11 (9), 1959–1962.
Papassotiropoulos, A., Streffer, J.R., Tsolaki, M., Schmid, S., Thal, D., Nicosia, F., Iakovidou, V., Maddalena, A., Lutjohann, D., Ghebremedhin, E., Hegi, T., Pasch, T., Traxler, M., Bruhl, A., Benussi, L., Binetti, G., Braak, H., Nitsch, R.M., Hock, C., 2003. Increased brain beta-amyloid load, phosphorylated tau, and risk of Alzheimer disease associated with an intronic CYP46 polymorphism. Arch. Neurol. 60 (1), 29–35.
Park, H.C., Kim, C.H., Bae, Y.K., Yeo, S.Y., Kim, S.H., Hong, S.K., Shin, J., Yoo, K.W., Hibi, M., Hirano, T., Miki, N., Chitnis, A.B., Huh, T.L., 2000. Analysis of upstream elements in the HuC promoter leads to the establishment of transgenic zebrafish with fluorescent neurons. Dev. Biol. 227 (2), 279–293.
Patten, S.A., Armstrong, G.A., Lissouba, A., Kabashi, E., Parker, J.A., Drapeau, P., 2014. Fishing for causes and cures of motor neuron disorders. Dis. Model. Mech. 7 (7), 799–809.
Peet, D.J., Turley, S.D., Ma, W., Janowski, B.A., Lobaccaro, J.M., Hammer, R.E., Mangelsdorf, D.J., 1998. Cholesterol and bile acid metabolism are impaired in mice lacking the nuclear oxysterol receptor LXR alpha. Cell 93 (5), 693–704.
Pereiro, P., Forn-Cuni, G., Dios, S., Coll, J., Figueras, A., Novoa, B., 2017. Interferon-independent antiviral activity of 25-hydroxycholesterol in a teleost fish. Antiviral Res. 145, 146–159.
Pfrieger, F.W., 2003. Role of cholesterol in synapse formation and function. Biochim. Biophys. Acta 1610 (2), 271–280.
Radhakrishnan, A., Ikeda, Y., Kwon, H.J., Brown, M.S., Goldstein, J.L., 2007. Sterol-regulated transport of SREBPs from endoplasmic reticulum to Golgi: oxysterols block transport by binding to Insig. Proc. Natl. Acad. Sci. U. S. A. 104 (16), 6511–6518.
Reschly, E.J., Ai, N., Welsh, W.J., Ekins, S., Hagey, L.R., Krasowski, M.D., 2008. Ligand specificity and evolution of liver X receptors. J. Steroid Biochem. Mol. Biol. 110 (1–2), 83–94.
Schols, L., Rattay, T.W., Martus, P., Meisner, C., Baets, J., Fischer, I., Jagle, C., Fraidakis, M.J., Martinuzzi, A., Saute, J.A., Scarlato, M., Antenora, A., Stendel, C., Hoflinger, P., Lourenco, C.M., Abreu, L., Smets, K., Paucar, M., Deconinck, T., Bis, D.M., Wiethoff, S., Bauer, P., Arnoldi, A., Marques, W., Jardim, L.B., Hauser, S., Criscuolo, C., Filla, A., Zuchner, S., Bassi, M.T., Klopstock, T., De Jonghe, P., Bjorkhem, I., Schule, R., 2017. Hereditary spastic paraplegia type 5: natural history, biomarkers and a randomized controlled trial. Brain 140 (12), 3112–3127.
Schonknecht, P., Lutjohann, D., Pantel, J., Bardenheuer, H., Hartmann, T., von Bergmann, K., Beyreuther, K., Schroder, J., 2002. Cerebrospinal fluid 24S-hydroxycholesterol is increased in patients with Alzheimer's disease compared to healthy controls. Neurosci. Lett. 324 (1), 83–85.
Shrivastava-Ranjan, P., Bergeron, E., Chakrabarti, A.K., Albarino, C.G., Flint, M., Nichol, S.T., Spiropoulou, C.F., 2016. 25-hydroxycholesterol inhibition of lassa virus infection through aberrant GP1 glycosylation. mBio 7 (6).

Sun, M.Y., Linsenbardt, A.J., Emnett, C.M., Eisenman, L.N., Izumi, Y., Zorumski, C.F., Mennerick, S., 2016. 24(S)-Hydroxycholesterol as a modulator of neuronal signaling and survival. Neuroscientist 22 (2), 132–144.

Testa, G., Staurenghi, E., Zerbinati, C., Gargiulo, S., Iuliano, L., Giaccone, G., Fanto, F., Poli, G., Leonarduzzi, G., Gamba, P., 2016. Changes in brain oxysterols at different stages of Alzheimer's disease: their involvement in neuroinflammation. Redox Biol. 10, 24–33.

Theofilopoulos, S., Abreu de Oliveira, W.A., Yang, S., Yutuc, E., Saeed, A., Abdel-Khalik, J., Ullgren, A., Cedazo-Minguez, A., Bjorkhem, I., Wang, Y., Griffiths, W.J., Arenas, E., 2019. 24(S), 25-Epoxycholesterol and cholesterol 24S-hydroxylase (CYP46A1) overexpression promote midbrain dopaminergic neurogenesis in vivo. J. Biol. Chem. 294 (11), 4169–4176.

Theofilopoulos, S., Griffiths, W.J., Crick, P.J., Yang, S., Meljon, A., Ogundare, M., Kitambi, S.S., Lockhart, A., Tuschl, K., Clayton, P.T., Morris, A.A., Martinez, A., Reddy, M.A., Martinuzzi, A., Bassi, M.T., Honda, A., Mizuochi, T., Kimura, A., Nittono, H., De Michele, G., Carbone, R., Criscuolo, C., Yau, J.L., Seckl, J.R., Schule, R., Schols, L., Sailer, A.W., Kuhle, J., Fraidakis, M.J., Gustafsson, J.A., Steffensen, K.R., Bjorkhem, I., Ernfors, P., Sjovall, J., Arenas, E., Wang, Y., 2014. Cholestenoic acids regulate motor neuron survival via liver X receptors. J. Clin. Invest. 124 (11), 4829–4842.

Theofilopoulos, S., Wang, Y., Kitambi, S.S., Sacchetti, P., Sousa, K.M., Bodin, K., Kirk, J., Salto, C., Gustafsson, M., Toledo, E.M., Karu, K., Gustafsson, J.A., Steffensen, K.R., Ernfors, P., Sjovall, J., Griffiths, W.J., Arenas, E., 2013. Brain endogenous liver X receptor ligands selectively promote midbrain neurogenesis. Nat. Chem. Biol. 9 (2), 126–133.

Trousson, A., Bernard, S., Petit, P.X., Liere, P., Pianos, A., El Hadri, K., Lobaccaro, J.M., Ghandour, M.S., Raymondjean, M., Schumacher, M., Massaad, C., 2009. 25-hydroxycholesterol provokes oligodendrocyte cell line apoptosis and stimulates the secreted phospholipase A2 type IIA via LXR beta and PXR. J. Neurochem. 109 (4), 945–958.

Tuong, Z.K., Lau, P., Du, X., Condon, N.D., Goode, J.M., Oh, T.G., Yeo, J.C., Muscat, G.E., Stow, J.L., 2016. RORalpha and 25-hydroxycholesterol crosstalk regulates lipid droplet homeostasis in macrophages. PLoS One 11 (1), e0147179.

Waltl, S., Patankar, J.V., Fauler, G., Nusshold, C., Ullen, A., Eibinger, G., Wintersperger, A., Kratky, D., Malle, E., Sattler, W., 2013. 25-Hydroxycholesterol regulates cholesterol homeostasis in the murine CATH.a neuronal cell line. Neurosci. Lett. 539, 16–21.

Wang, F., Xia, W., Liu, F., Li, J., Wang, G., Gu, J., 2012. Interferon regulator factor 1/retinoic inducible gene I (IRF1/RIG-I) axis mediates 25-hydroxycholesterol-induced interleukin-8 production in atherosclerosis. Cardiovasc. Res. 93 (1), 190–199.

Wolf, G., 1999. The role of oxysterols in cholesterol homeostasis. Nutr. Rev. 57 (6), 196–198.

Yamanaka, K., Saito, Y., Yamamori, T., Urano, Y., Noguchi, N., 2011. 24(S)-hydroxycholesterol induces neuronal cell death through necroptosis, a form of programmed necrosis. J. Biol. Chem. 286 (28), 24666–24673.

Zhang, J., Liu, Q., 2015. Cholesterol metabolism and homeostasis in the brain. Protein Cell 6 (4), 254–264.